

# Structure formation and properties of biaxially oriented polyethylene films by compression of injected mouldings

F. Ania and F. J. Baltá Calleja\*

*Instituto de Estructura de la Materia, CSIC, c/Serrano 119, 28006-Madrid, Spain*

and R. K. Bayer

*Institut für Werkstofftechnik, Universität GH Kassel, Wilhelmshöher Allee 73,*

*D-3500 Kassel, Germany*

*(Received 31 December 1990; revised 19 February 1991; accepted 12 March 1991)*

The crystal orientation and the microstructure of biaxially oriented polyethylene films are examined by means of wide (WAXS) and small angle X-ray scattering (SAXS) as a function of the final applied pressure. The SAXS patterns of the starting uniaxially oriented injection moulded materials, having a shish-kebab microstructure, yield two meridional maxima with long periods of 36 and  $\sim 50$  nm. It is shown that with increasing applied compressive stresses the intensity of the initial meridional long period decreases, while a new equatorial long period appears in the normal direction to the initial orientation. This final long period only depends on the temperature of deformation. Results are discussed in terms of a gradual transformation from the original shish-kebab structure into oriented domains of the pressure-induced structure, appearing at right angles to the initial axial direction. The coexistence of microdomains, with chain and lamellar orientation at right angles to each other, yields tensile strength values in the two principal directions of the films which are larger than 100 MPa.

(Keywords: polyethylene; compressive deformation; biaxial orientation; WAXS; SAXS; tensile strength)

## INTRODUCTION

Several solid state processing techniques have been developed to improve polymer properties through increasing their molecular deformation. Among some of the most commonly used are tensile drawing, hydrostatic extrusion, die drawing, rolling and rolltrusion<sup>1-4</sup>. Most of these techniques introduce either uniaxial or biaxial orientation into the deformed material. In a recent investigation an alternative mode of processing polyethylene (PE) into biaxially oriented 0.1–0.2 mm thick films following a two-step process has been described<sup>5</sup>. Accordingly, the materials were injection moulded into uniaxially oriented rods and then pressed in a direction perpendicular to the previous injection flow. The characterization of the strain for the compressed biaxially oriented films in the three main directions has been recently reported<sup>5</sup>. In addition, the compressive stress-strain behaviour of these biaxially oriented PE films has been described with the aid of a modified Van der Waals equation of state for real networks<sup>6</sup>. Comparison of experimental and calculated data with this concept supports the view that the network of entanglements, which is transferred from the melt into the solid state, is preserved even after very large deformations. The analysis of the data supports the view that the segment length of this network is close to the value of the X-ray long spacing of the initial oriented structure. The aim of the present work is to supplement our previous investigation and

characterize the changes in crystal orientation and microstructure of the biaxially oriented films as revealed by X-ray scattering techniques as a function of final applied pressure ( $P_f$ ) and deformation temperature ( $T_d$ ). Additionally, the mechanical properties of the biaxially drawn films (draw ratio, ultimate tensile strength) will be discussed in the light of the morphological observations.

## EXPERIMENTAL

Highly oriented injected mouldings were used as precursors for the compression experiments. The material employed was linear PE, Lupolen 6021 D, having a weight average molecular weight,  $\bar{M}_w = 182\,000$  and a number average molecular weight,  $\bar{M}_n = 25\,000$ . The mouldings were produced following a method that enhances axial elongational flow during the filling stage<sup>7</sup>. This method yields a high degree of uniaxial orientation in the mouldings; largest orientations being obtained for the lowest injection temperatures. The influence of mould geometry and processing parameters on the physical properties of the uniaxially oriented materials were previously reported<sup>8-10</sup>. In the present study the oriented injection moulded precursors had a square cross-section of  $4 \times 4$  mm<sup>2</sup> and the injection melt temperature was 148°C. Figure 1 illustrates a characteristic birefringence profile measured perpendicularly to the long axis of one injection moulding. A profile with a high average value of optical birefringence,  $\Delta n = 40 \times 10^{-3}$ , is observed. The uniaxially oriented samples were cut to a fixed length

\* To whom correspondence should be addressed

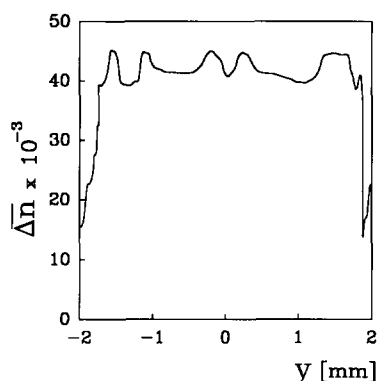


Figure 1 Birefringence profile, measured along the  $y$ -axis, of an investigated elongational flow injection moulded sample ( $T_m = 148^\circ\text{C}$ )

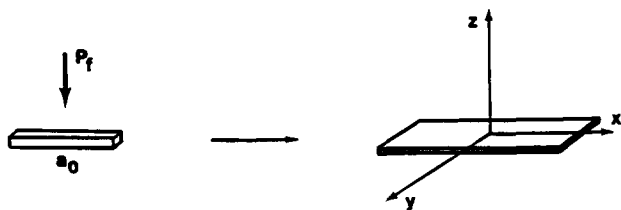


Figure 2 Schematics of the sample dimensions before and after compression. The compressive force,  $P_x$ , is directed along the  $z$ -axis

$a_0 = 56$  mm. These segments were placed between the plates of a press at two different  $T_d$  values lower than the melting point of the material ( $120$  and  $127^\circ\text{C}$ ). Compression, using forces between  $30$  kN and  $600$  kN, was perpendicularly applied to the former injection axis. The pressing time was  $20$  s in all cases. After compression, biaxially deformed  $0.1$ – $0.2$  mm thick films were obtained. Further experimental details are given elsewhere<sup>5</sup>.

Figure 2 schematically shows the ideal case of a rod of length  $a_0$  which is transformed into a film after undergoing an homogeneous orthogonal biaxial deformation. The non-linearity of the deformation causes, however, a drawn rectangular frame to be transformed into an elliptical one. For the sake of simplicity, if we restrict ourselves to the discussion of the central part of the biaxial films, we can assume to be dealing with a quasi-orthogonal biaxial deformation, which justifies the approximation made in Figure 2.

For the measurement of the tensile strength, the samples were cut into dumb-bell shaped strips (width  $3$  mm and gauge length  $30$  mm). The test specimens were stretched at room temperature in an Instron machine at a rate of  $20$  mm  $\text{min}^{-1}$ . In these biaxially drawn films the measurement of the tensile strength along the  $y$  and  $x$  directions was carried out independently.

Wide (WAXS) and small angle X-ray scattering (SAXS) experiments were performed at room temperature with a point collimation Kiessig camera and a Rigaku rotating anode X-ray generator. Sample–film distances of  $50$  and  $500$  mm were used. Ni-filtered Cu- $K\alpha$  radiation was employed.

## RESULTS AND DISCUSSION

### Crystal orientation

Figure 3 shows the WAXS patterns of the obtained films which strongly depend on the final applied pressure

$P_f$ . The starting uniaxially oriented material shows a highly oriented fibre structure (Figure 3a). In over-exposed photographs of these uniaxially oriented materials, there is a faint  $(0\ 0\ 1)$  triclinic reflection. This implies that after the injection process, and owing to the stress applied to the polymer, a small amount of material may undergo twist disclinations which give rise to this new crystal modification<sup>11</sup>. The occurrence of a modification, other than the orthorhombic one, has been previously reported for biaxially stretched PE<sup>12</sup>. After compression, two main effects in the WAXS pattern of the biaxially oriented films are immediately distinguished (Figures 3b–d): the first is the intensity loss of the  $(2\ 0\ 0)$  and  $(0\ 2\ 0)$  spots (the latter are not shown), which suggests that some new modes of planar orientation of crystals are being induced by means of compression<sup>13</sup>; the second is the progressive appearance of a new intensity maximum of the  $(1\ 1\ 0)$  reflection on the meridian, together with a concurrent intensity loss of this reflection on the equator.

To analyse more quantitatively this transformation, we have plotted in Figure 4 the relative azimuthal intensity distribution of the  $(1\ 1\ 0)$  reflection as a function of final applied pressure. At  $P_f = 0$  MPa the scattering intensity is concentrated on the equator ( $\phi = 90^\circ$ ). At  $15$  MPa a significant amount of scattered intensity on the meridian ( $\phi = 0^\circ$ ) is observed, while the shape of the intensity distribution around the equator is hardly affected. At  $50$  MPa, however, the intensity maximum in the equatorial direction, corresponding to the initial crystal structure, becomes smaller and the intensity distribution becomes broader at the expense of the newly created crystal orientation. On the other hand, the analysis of the radial integral breadth shows that in the equatorial direction the coherently diffracting

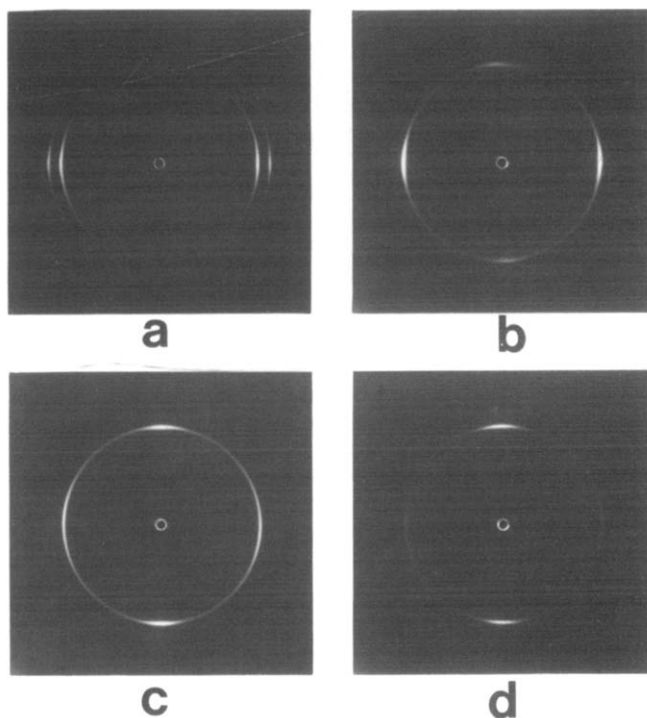
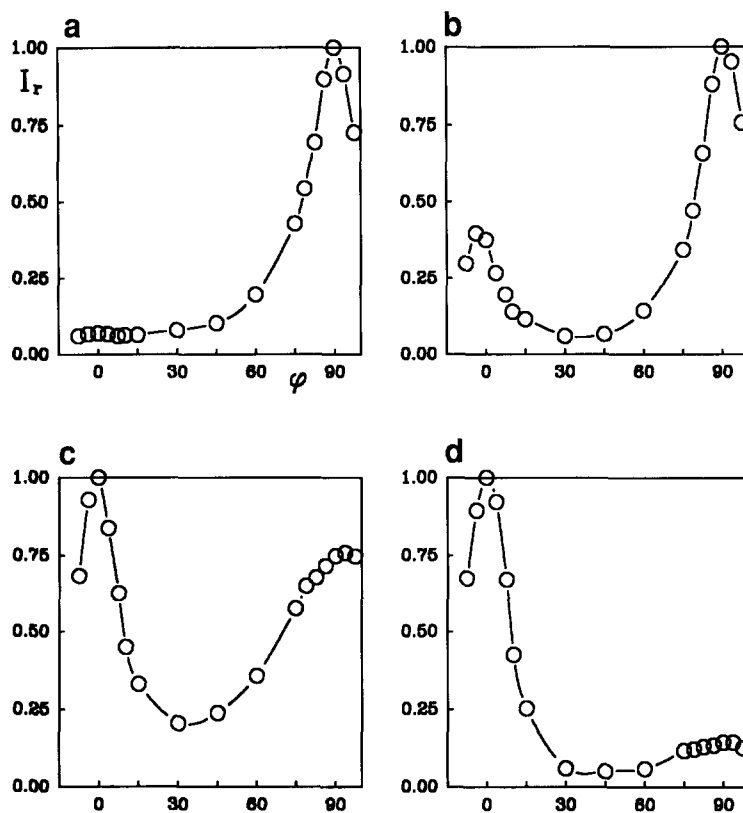
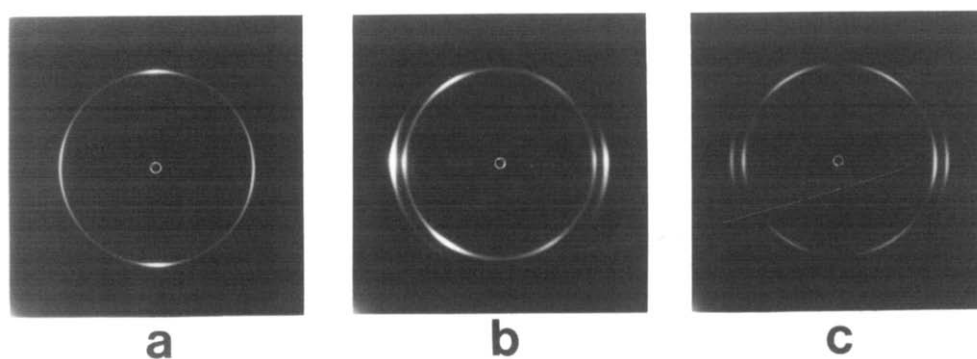


Figure 3 WAXS photographs of the investigated PE samples as a function of  $P_f$ . X-ray beam is perpendicular to the film surface. Injection direction: vertical. (a) Initial uniaxial material,  $P_f = 0$  MPa; (b)  $P_f = 15$  MPa; (c)  $P_f = 50$  MPa; (d)  $P_f = 135$  MPa



**Figure 4** Azimuthal intensity distribution of the (1 1 0) reflection of the same samples as in Figure 3 as a function of  $P_t$  ( $\phi = 0$ , meridional direction): (a) 0 MPa; (b) 15 MPa; (c) 50 MPa; (d) 135 MPa



**Figure 5** X-ray photographs along the three principal directions of the PE film pressed at  $P_t = 50$  MPa. X-ray beam is perpendicular to: (a) xy plane (x-axis vertical); (b) xz plane (x-axis vertical); (c) yz plane (y-axis vertical)

crystalline regions of the initial structure are larger ( $D_{110} \approx 19$  nm) than the average size of the crystalline blocks within the new structure ( $D_{110} \approx 14$  nm). These results indicate that at this stage of deformation, the crystallites, which appear at right angles, are smaller but with a higher degree of orientation than the initial ones. Finally, at a pressure of 135 MPa, the majority of the crystalline material shows the meridional orientation while only very little of the former crystal orientation remains.

We will next focus our attention on the case of  $P_t = 50$  MPa, in which the material shows nearly the same amount of intensity distributed in the two orthogonal directions, to examine in detail the crystalline structure of this material. In a biaxially oriented sample, the complete analysis of the texture patterns requires, in general, to take a number of X-ray photographs to cover

all possible ranges of orientation in small angular steps. However, in our particular case because of the existing predominant orthorhombic symmetry, the axes of the macroscopic sample, the principal directions of deformation and the unit cell orientation can be easily related. Hence, in this case to characterize the structure it is sufficient to take three photographs along the three principal directions. Figure 5a shows the X-ray photograph with the primary beam perpendicular to the xy plane (x coincides with the injection flow axis). Figures 5b and c correspond to the other two perpendicular directions. In the latter two cases a maximum of intensity of the (1 1 0) reflection appears on the equator, along with a pair of secondary maxima at  $\sim 60^\circ$  from the equator. These photographs can be compared with the X-ray patterns of the well-known doubly oriented structure obtained by rolling PE,

previously reported by Hay and Keller<sup>14</sup> and by Meinel and Peterlin<sup>15</sup>. In this case, it is known that the c-axis of the unit cell is roughly oriented in the rolling direction and one set of (1 1 0) planes is parallel to the rolling plane, whereas two other sets of lattice planes are oriented at equal angles about z. A possible explanation for the results is to assume that in our material there is a juxtaposition of microdomains having a doubly oriented crystal structure<sup>16</sup> (similar to that reported by Hay and Keller<sup>14</sup>), i.e. new domains having a pressure induced fibrillar structure rotated 90° with respect to the initial fibre structure. In the latter case the c-axis is oriented along the previous injection direction, while in the former type of domains the molecular chains are orthogonal to that direction. We will denote such a structure as 'doubly oriented biaxial structure'.

**Microstructure**

The morphology of the starting uniaxially oriented injection moulded material is known to be one of interlocking shish-kebabs<sup>17,18</sup>, i.e. extended chain fibrils (nuclei) and perpendicular lamellae grown epitaxially in the row nuclei<sup>19,20</sup>. This morphology is practically the same as that first reported by Odell *et al.* for melt extruded filaments of PE<sup>19,21,22</sup>. Figure 6a shows the SAXS pattern corresponding to such a uniaxial structure. This pattern presents two well defined intensity maxima in the axial direction. The outer maximum, which corresponds to a long period  $L = 36$  nm, can be related to the average distance between chain folded lamellar kebabs. The inner maximum could be associated to some characteristic periodicity along the interlocking shish-kebab fibre structure. The application of a compressive stress normal to the oriented rods results in the appearance of a new SAXS maximum at right angles to the direction of the previous injection flow (Figures

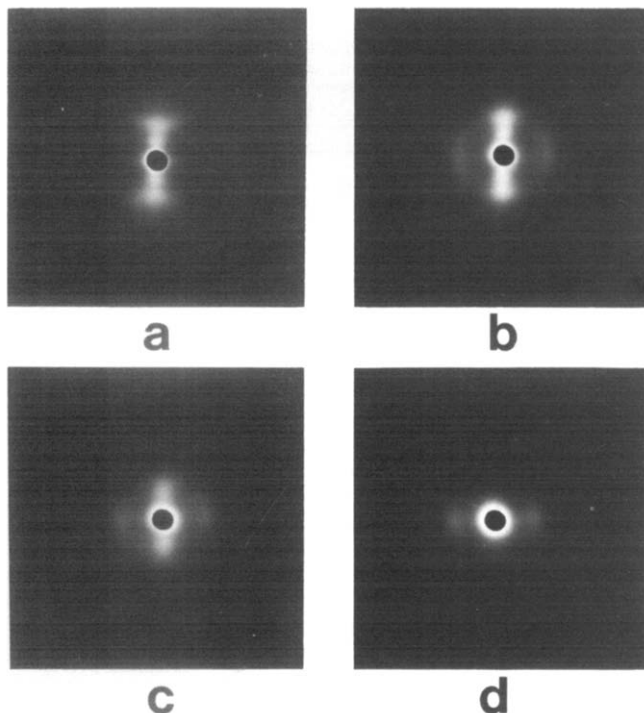


**Figure 6** SAXS patterns of the investigated PE samples as a function of  $P_f$ . X-ray beam is perpendicular to the film surface. Injection direction: vertical. (a) Initial uniaxial material,  $P_f = 0$  MPa; (b)  $P_f = 15$  MPa; (c)  $P_f = 50$  MPa; (d)  $P_f = 135$  MPa

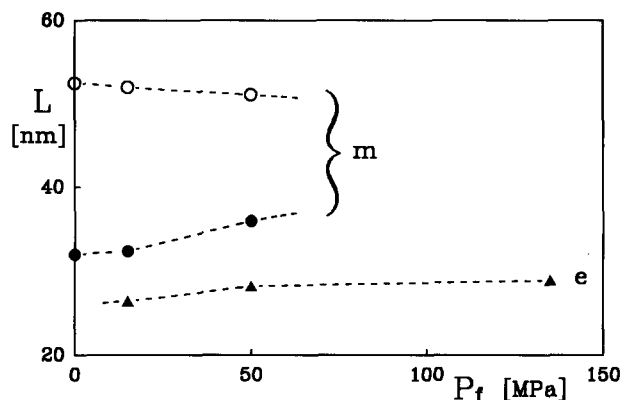


**Figure 7** Long spacings of the biaxially oriented films, in the meridional (m) and in the equatorial (e) direction, as a function of  $P_f$  (see Figure 6)

**Table 1** Meridional ( $L_m$ ) and equatorial ( $L_e$ ) long spacings, with X-rays perpendicular to the xy, xz and yz planes, of a biaxially oriented PE film at  $P_f = 50$  MPa

	xy	xz	yz
$L_m$ (nm)	51	49	-
	36	37	28
$L_e$ (nm)	28	-	-

6b-d). We will see below that the highest deformation in the press takes place precisely in that direction. To analyse these changes, we have plotted in Figure 7 the observed long spacing, both in the meridional and in the equatorial direction, as a function of applied pressure. It can be seen that the characteristic initial double maximum is preserved up to a certain pressure, between 50 MPa and 100 MPa. Simultaneously one also observes the rapid appearance of an equatorial scattering maximum, corresponding to the new fibrillar structure. From these findings we conclude that the original shish-kebab structure is preserved up to pressures above 50 MPa, whereas at 135 MPa only some very faint scattering is still present in the meridional direction. The value of the long spacing does not appreciably change with pressure, though a certain increasing tendency could be attributed either to annealing effects or to temperature changes within the samples during rapid compressive deformation<sup>23</sup>.

We wish to analyse in more detail the microstructure of the material deformed at a final pressure of 50 MPa. Figure 8 shows SAXS photographs taken along the three principal directions for this particular PE film. The corresponding long spacings are given in Table 1. Figure 8a illustrates again the meridional and equatorial SAXS maxima corresponding, respectively, to the original uniaxially oriented structure and to the compression-induced fibrillar one. Figure 8b shows only the maxima corresponding to the original shish-kebab microstructure together with an additional equatorial continuous scattering. The latter scattering can be associated with the presence of longitudinal microvoids parallel to the new fibrillar structure. On the other hand, Figure 8c shows the equatorial maximum associated with the compression-induced structure parallel to the y-axis (vertical), together with a very strong scattering (in the

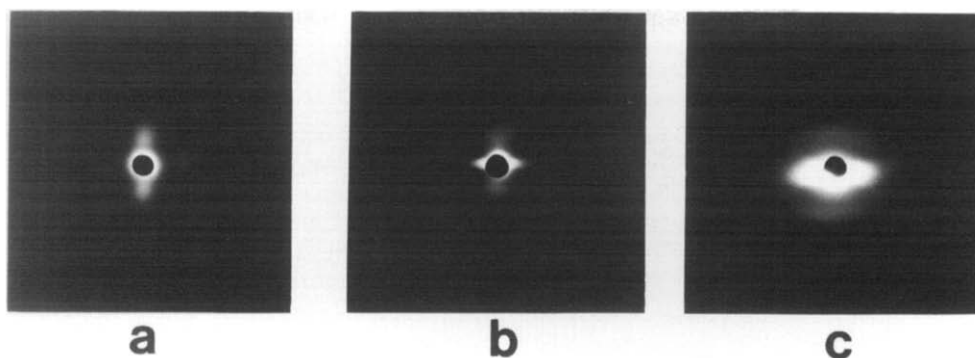


**Figure 8** SAXS patterns along the three principal directions of the PE film pressed at  $P_f = 50$  MPa. The corresponding long spacings are given in Table 1. The X-ray beam direction in (a), (b) and (c) is the same as in Figure 5

z direction). In this case the continuous scattering can be attributed to the presence of microvoids parallel to the shish-kebab fibrils<sup>11</sup>. The above results are in support of the concept of microdomains containing the original oriented structure which are coexisting with regions of the new pressure-induced fibre-like structure which emerges at right angles to the former orientation direction. According to the model of plastic deformation proposed by Peterlin<sup>16</sup>, the appearance of the new long period might be connected with a discontinuous process in which microfibrils are pulled out at right angles to the initial shish-kebab structure and these fibrils tend to coalesce into new fibrillar domains having a molecular orientation normal to the initial orientation. In other words, after compression we have a structure of microdomains where the lamellar normals to each one of the two structures, are orthogonal. Such a composite superstructure is a consequence of the heterogeneous nature of the deformation mechanism at high temperature, as recently evidenced by transmission electron microscopy (TEM) of drawn thin films having an initial shish-kebab structure<sup>24</sup>. The coexistence of two differently oriented structures has also been reported in rolled PE<sup>15,25,26</sup> and in the second drawing of uniaxially oriented films<sup>27</sup>. The specific distribution of domains within the sample is still an open question which should be further investigated by electron microscopy.

Another interesting aspect of our compression experiments is the fact that the value of the long spacing, appearing in the equatorial direction, is independent of parameters such as molecular weight, initial state of the material, dimensions of the sample or applied pressure. In fact,  $L$  seems to be a unique function of  $T_d$ , as previously observed in the case of uniaxial deformation of PE<sup>28</sup>. Figure 9 shows the good agreement between the average values obtained at two different compression temperatures for our series of compressed films with the experimental findings of Corneliussen and Peterlin for uniaxially deformed PE<sup>28</sup>. Similar results have also been reported by Bessel and Young<sup>29</sup> showing that  $L$  of compression-oriented PE only depends on  $T_d$ .

#### Mechanical properties

The compression behaviour of the biaxial films greatly depends on the initial orientation of the injected materials. Figure 10 shows the macroscopic draw ratios,  $\lambda$ , along the two principal directions of the series of deformed films, as a function of  $P_f$ . For the discussion below it is convenient to define  $\lambda$ , along any particular

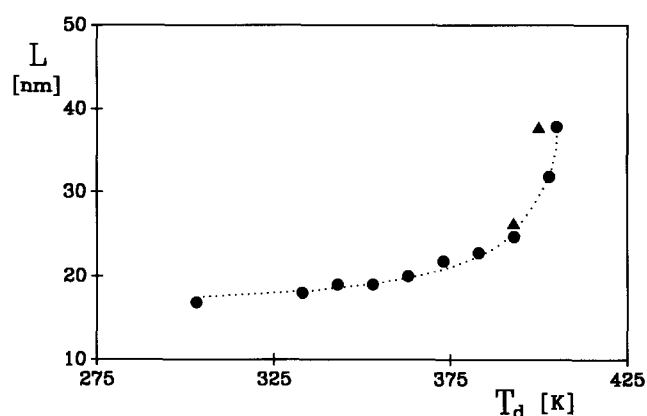


**Figure 9** Long spacing as a function of  $T_d$ : (●) experimental data of Corneliussen and Peterlin for uniaxially drawn PE<sup>28</sup>; (▲) biaxially oriented PE films investigated in this work

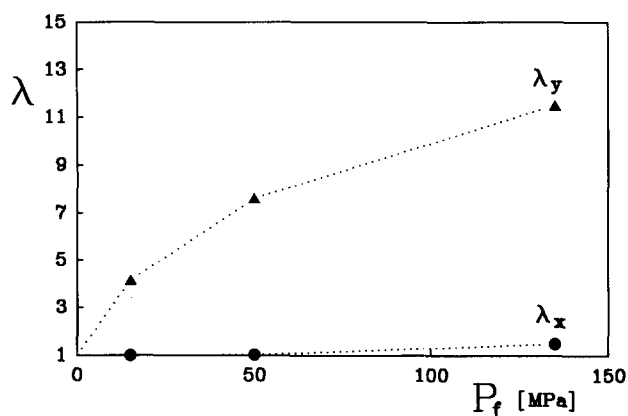


**Figure 10** Macroscopic draw ratio,  $\lambda$ , along the two principal directions of the film plane, x and y, as a function of  $P_f$

direction, as the quotient of the resulting film length, after removing the pressure, to the initial length in that direction. It is observed that deformation in the x-axis direction is strongly hindered as compared to the perpendicular direction. This is due to, both, the initial anisotropy ( $A_0 = a_0/b_0 \sim 13$ , Figure 2) of the initial injected rods<sup>5</sup>. Hence, the material flow in the y direction, already occurring at very low pressures, gives rise to the newly created oriented fibrous domains in that direction.

From the point of view of application, the main interest of a biaxially oriented film lies in the possibility of having

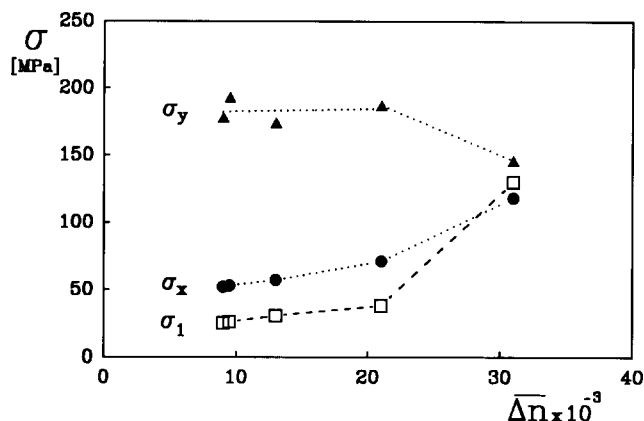


**Figure 11** Tensile strength,  $\sigma$ , along the two principal directions,  $x$  and  $y$ , of the biaxially oriented PE films as a function of initial orientation;  $\sigma_1$  is the tensile strength of the initial uniaxial rods measured in the injection direction ( $x$ -axis)

an improved mechanical response in any direction of the film plane. *Figure 11* shows the tensile strength of a series of biaxially deformed films, in the  $x$  and  $y$  directions, as a function of initial orientation ( $\Delta n$ ), the latter being a reciprocal function of the injection melt temperature. These data correspond to a series of PE samples (Vestolen A 6012), with  $\bar{M}_w = 108\,000$ , which were pressed at  $127^\circ\text{C}$ . We have also plotted the tensile strength values,  $\sigma_1$ , for the initial uniaxial rods which were measured in the injection direction. In this case the whole rods were used as test specimens. It is known that at high injection melt temperatures ( $T_m > 180^\circ\text{C}$ ) the resulting injected material remains almost isotropic ( $\Delta n < 15 \times 10^{-3}$ )<sup>8</sup>. Therefore the  $\sigma_1$  values, shown in *Figure 11* for this material, are not far from the typical values of unoriented low molecular weight PE ( $\sim 25$  MPa). By lowering  $T_m$  one obtains fibre self-reinforced materials, with improved orientation ( $\Delta n \sim 30 \times 10^{-3}$ ), yielding, as a result, tensile strength values<sup>8</sup> larger than 100 MPa. After compression, the biaxially oriented films resulting from those rods which had a lower initial orientation (lower birefringence), show a dramatic increase in  $\sigma_y$  but only a moderate one in the former injection direction ( $\sigma_x$ ). On the contrary, due to the persistence of the original fibre structure within the highly oriented biaxial films, tensile strength values larger than 100 MPa in the two principal directions of the film plane can be obtained. Thus, the present mode of processing yields a material with enhanced mechanical properties in all directions of the film surface.

## CONCLUSIONS

1. By pressing uniaxially oriented PE rods in a direction normal to the  $c$  axis, films showing a doubly oriented biaxial structure are obtained.
2. For a given range of applied pressure, the analysis of SAXS data reveals the coexistence of the initial shish-kebab oriented structure with a newly created

fibre-like structure appearing at right angles to the former direction.

3. Similarly, as in the case of uniaxially stretched materials,  $L$  of the new fibre structure is independent of the initial structure, and is only a unique function of  $T_d$ .
4. Stress-strain analysis carried out along the two principal directions of the surface of the biaxially oriented films yield, in both directions, tensile strength values which are four to five times larger than in conventionally processed unoriented PE.

## ACKNOWLEDGEMENT

Grateful acknowledgement is due to CICYT, Spain, for the support of this investigation (grant MAT88-0159).

## REFERENCES

- 1 Zachariades, A. E. and Porter, R. S. (Eds) 'The Strength and Stiffness of Polymers', Marcel Dekker, New York, 1983
- 2 Hallam, M. A., Cansfield, D. L. M., Ward, I. M. and Pollard, G. *J. Mater. Sci.* 1986, **21**, 4199
- 3 Kanamoto, T., Tsuruta, A., Tanaka, K., Takeda, M. and Porter, R. S. *Polymer* 1983, **15**, 327
- 4 Magill, J. H. *19th EPS Conf. on Macromol. Phys. Conf. Abstr.* 1988, **12D**, 63
- 5 Ania, F., Bayer, R. K. and Baltá Calleja, F. J. *Int. Polym. Proc.* in press
- 6 Kilian, H. G., Schrödi, W., Ania, F., Bayer, R. K. and Baltá Calleja, F. J. *Coll. Polym. Sci.* 1991, **269**, 859
- 7 Bayer, R. K. *14th EPS Conf. Macromol. Phys. Conf. Abstr.* 1982, **6G**, 75
- 8 López Cabarcos, E., Bayer, R. K., Zachmann, H. G., Baltá Calleja, F. J. and Meins, W. *Polym. Eng. Sci.* 1989, **29**, 193
- 9 Bayer, R. K., Baltá Calleja, F. J., López Cabarcos, E., Zachmann, H. G., Paulsen, A., Brüning, F. and Meins, W. *J. Mater. Sci.* 1989, **24**, 2643
- 10 Rueda, D. R., Bayer, R. K., Baltá Calleja, F. J. and Zachmann, H. G. *J. Macromol. Sci. Phys.* 1989, **B28**, 265
- 11 Zwijnenburg, A., van Hutten, F., Pennings, A. J. and Chanzy, H. D. *Coll. Polym. Sci.* 1978, **256**, 729
- 12 Adams, G. C. *J. Polym. Sci. A2* 1971, **9**, 1235
- 13 Sakai, Y. and Miyasaka, K. *Polymer* 1988, **29**, 1608
- 14 Hay, L. and Keller, A. *J. Mater. Sci.* 1966, **1**, 41
- 15 Meinel, G. and Peterlin, A. *Kolloid Z.Z. Polym.* 1970, **242**, 1151
- 16 Peterlin, A. *Coll. Polym. Sci.* 1987, **265**, 357
- 17 Heckmann, W. *PhD Thesis* Technische Hochschule Darmstadt, 1976
- 18 Ehrenstein, G. W. and Martin, C. *Kunststoffe* 1985, **75**, 105
- 19 Odell, J. A., Grubb, D. T. and Keller, A. *Polymer* 1978, **19**, 617
- 20 Hoffmann, J. D. *J. Res. Natl. Bur. Stand.* 1979, **84**, 359
- 21 Bashir, Z., Odell, J. A. and Keller, A. *J. Mater. Sci.* 1984, **19**, 3713
- 22 Bashir, Z., Odell, J. A. and Keller, A. *J. Mater. Sci.* 1986, **21**, 3993
- 23 Rodriguez, E. L. and Filisko, F. E. *Polym. Eng. Sci.* 1986, **26**, 1060
- 24 Brady, J. M. and Thomas, E. L. *J. Mater. Sci.* 1989, **24**, 3319
- 25 de Candia, F., Vittoria, V., Rizzo, G. and Titomanlio, G. *J. Macromol. Sci. Phys.* 1986, **B25**, 365
- 26 de Candia, F., Romano, G., Vittoria, V., Rizzo, G. and Titomanlio, G. *J. Macromol. Sci. Phys.* 1989, **B28**, 503
- 27 Hinrichsen, G., Eberhardt, A., Lippe, U. and Springer, H. *Coll. Polym. Sci.* 1981, **259**, 73
- 28 Corneliussen, R. and Peterlin, A. *Makromol. Chem.* 1967, **105**, 193
- 29 Bessel, T. and Young, R. J. *J. Polym. Sci.* 1974, **B12**, 629